



This is a repository copy of *Multiple Source Adaptive Active Noise and Vibration Control*.

White Rose Research Online URL for this paper:  
<http://eprints.whiterose.ac.uk/80876/>

---

**Monograph:**

Tokhi, M.O., Mamour, K. and Hossain, M.A. (1996) Multiple Source Adaptive Active Noise and Vibration Control. Research Report. ACSE Research Report 644 . Department of Automatic Control and Systems Engineering

---

**Reuse**

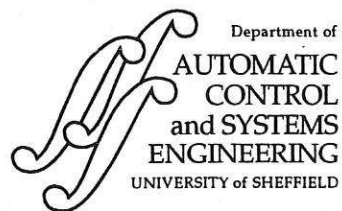
Unless indicated otherwise, fulltext items are protected by copyright with all rights reserved. The copyright exception in section 29 of the Copyright, Designs and Patents Act 1988 allows the making of a single copy solely for the purpose of non-commercial research or private study within the limits of fair dealing. The publisher or other rights-holder may allow further reproduction and re-use of this version - refer to the White Rose Research Online record for this item. Where records identify the publisher as the copyright holder, users can verify any specific terms of use on the publisher's website.

**Takedown**

If you consider content in White Rose Research Online to be in breach of UK law, please notify us by emailing [eprints@whiterose.ac.uk](mailto:eprints@whiterose.ac.uk) including the URL of the record and the reason for the withdrawal request.



[eprints@whiterose.ac.uk](mailto:eprints@whiterose.ac.uk)  
<https://eprints.whiterose.ac.uk/>



## **MULTIPLE SOURCE ADAPTIVE ACTIVE NOISE AND VIBRATION CONTROL**

**M O Tokhi<sup>\*</sup>, K Mamour<sup>\*</sup> and M A Hossain<sup>\*\*</sup>**

<sup>\*</sup> Department of Automatic Control and Systems Engineering,  
The University of Sheffield, Mappin Street, Sheffield, S1 3JD, UK.

<sup>\*\*</sup> Department of Computer Science, University of Dhaka, Bangladesh.

Tel: + 44 (0)114 282 5136.  
Fax: + 44 (0)114 273 1729.  
E-mail: O.Tokhi@sheffield.ac.uk.

Research Report No. 644

October 1996

## Abstract

This report presents an investigation into the development of an adaptive active control strategy for noise cancellation and vibration suppression using a multi-source configuration. A self-tuning control algorithm is developed on the basis of optimum cancellation of broadband noise/vibration at a set of observation points. The algorithm is implemented on a digital processor and its performance assessed in the cancellation of noise in a free-field medium and the suppression of vibration in a flexible beam structure.

*Key words: Active control, active noise control, active vibration control, adaptive control, self-tuning control.*

**CONTENTS**

|                                      |     |
|--------------------------------------|-----|
| Title                                | i   |
| Abstract                             | ii  |
| Contents                             | iii |
| List of figures                      | iv  |
| 1 Introduction                       | 1   |
| 2 Active noise control               | 3   |
| 2.1 Self-tuning active noise control | 7   |
| 2.2 Simulation algorithm             | 15  |
| 2.3 Implementation and results       | 16  |
| 3 Active vibration control           | 21  |
| 3.1 Simulation algorithm             | 22  |
| 3.2 Implementation and results       | 23  |
| 4 Conclusion                         | 28  |
| 5 References                         | 28  |

## LIST OF FIGURES

- Figure 1: Active noise control structure;  
(a) Schematic diagram. (b) Block diagram.
- Figure 2: Self-tuning active controller.
- Figure 3: Frequency response measurement.
- Figure 4: Block diagram of the simulated feedforward ANC structure.
- Figure 5: Transfer characteristics of loudspeaker-microphone combination;  
(a) System gain. (b) System phase.
- Figure 6: Cancelled spectrum at the observation point with the SISO self-tuning ANC system.
- Figure 7: Cancelled spectrum with the SIMO self-tuning ANC system;  
(a) Observation point 1. (b) Observation point 2.
- Figure 8: Active vibration control structure.
- Figure 9: Cancelled spectrum with the SISO self-tuning AVC system at the observation point.
- Figure 10: Average autopower spectral densities along the beam before and after cancellation with the SISO self-tuning AVC system. ✓
- Figure 11: Attenuated spectrum of the disturbance with the SIMO self-tuning AVC system;  
(a) At observation point 1. (b) At observation point 2.
- Figure 12: Average autopower spectral densities along the beam before and after cancellation with the SIMO self-tuning AVC system. ✓

## 1 INTRODUCTION

Active control of noise/vibration consists of artificially generating cancelling source(s) to destructively interfere with the unwanted source and thus result in a reduction in the level of the noise/vibration at desired location(s). Active noise/vibration control is not a new concept. It is based on the principles that were initially proposed by Lueg in the early 1930s for noise cancellation (Lueg, 1936). Since then a considerable amount of research work has been devoted to the development of methodologies for the design and realisation of active noise/vibration control (active control) systems in various applications (Guicking, 1993; Leitch and Tokhi, 1987; Leventhal, 1980; Warnaka, 1982).

Active control is realised by detecting and processing the noise/vibration (disturbances) by a suitable electronic controller so that, when superimposed on the disturbances, cancellation occurs. Due to the broadband nature of these disturbances, it is required that the control mechanism realises suitable frequency-dependent characteristics so that cancellation over a broad range of frequencies is achieved (Leitch and Tokhi, 1987; Tokhi and Leitch, 1991a). In practice, the spectral contents of these disturbances as well as the characteristics of system components are in general subject to variation, giving rise to time-varying phenomena. This implies that the control mechanism is further required to be intelligent enough to track these variations, so that the desired level of performance is achieved and maintained.

Through his experiments of reducing transformer noise, Conover was the first to realise the need for a 'black box' controller that would adjust the cancelling signal in accordance with information gathered at a remote distance from the transformer (Conover, 1956). Later it has been realised by numerous researchers that an essential requirement for an active noise/vibration control system to be practically successful is to have an adaptive capability (Burgess, 1981; Chaplin, 1980; Elliott and Nelson, 1986; Elliott *et al.*, 1987b; Leitch and Tokhi, 1987; Ross, 1982). Implementing an adaptive control algorithm within an active control system will allow the controller characteristics to be adjusted in accordance to changes in the system.

Chaplin and his associates have reported some success with an adaptive scheme based on a trial and error waveform generation (Chaplin, 1980, 1983; Chaplin and Smith, 1981; Chaplin *et al.*, 1987). Their method relies on the source noise being periodic. The method has been tested with rotary machines such as motor vehicle, fan, etc. where the noise spectrum is harmonically related to the fundamental (engine firing) frequency. The engine firing frequency provides a clock signal to the algorithm. Noticeable amount of theoretical and practical investigations have subsequently been reported in the area of adaptive active control (Clark and Fuller, 1991; Dines, 1982; Elliott and Nelson, 1986; Elliott *et al.*, 1987b; Eriksson *et al.*, 1987, 1988; Fuller *et al.*, 1992; Roure, 1985; Roure and Nayroles, 1984; Sjosten, 1985; Snyder and Hansen, 1992; Tokhi and Leitch, 1989, 1991b). Among these the scheme developed by Eriksson and his co-workers relies on the development of a model of the source. The scheme reported by Nelson, Elliott and co-workers is based on minimisation (in the least square sense) of sound level at discrete locations in the medium. The control scheme reported by Tokhi and Leitch is based on optimum cancellation of disturbances. The work reported here extends the latter to incorporate multiple cancelling sources.

Active control mechanisms developed generally concentrate on reducing the level of the disturbances at selective frequencies or at narrow bands. In doing so, problems related to observation and/or control spill-over due to un-modelled dynamics of the system arise. These problems can be avoided by designing an active control system that incorporates a suitable system identification algorithm through which an appropriate model of the system can be developed within a broad frequency range of interest. The active control system presented in this report includes an on-line system identification algorithm which gives a suitable model of the system in parametric form within a broad range of frequencies of interest. The model thus obtained is then used to design the required controller and generate the corresponding control signal so that to reduce the level of the disturbances over this broad frequency range.

It is important to note that, the superposition of the component waves in an active control system results in an interference pattern throughout the medium in which the level

of cancellation in some regions will be higher and in some regions it will be lower or even will correspond to a reinforcement. The level and physical extent of cancellation achieved is primarily dependent on the geometrical arrangement of system components. Moreover, the number of secondary sources, depending on limitations due to physical dimensions, has a significant effect on the level as well as physical extent of cancellation.

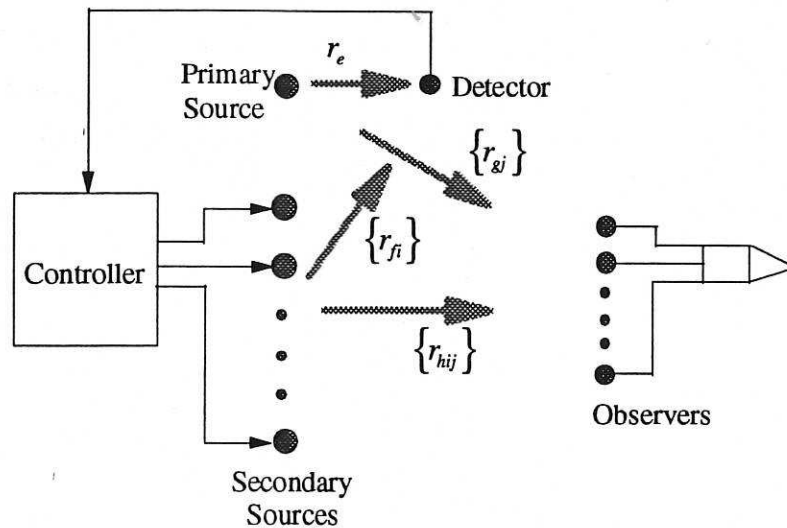
This report presents an investigation into the development of an active control mechanism for noise cancellation and vibration suppression within an adaptive control framework. An active noise control (ANC) system is designed utilising a single-input multi-output (SIMO) control structure to yield optimum cancellation of broadband noise, emanating from a point source, at a set of observation points in a three-dimensional propagation medium. The controller design relations are formulated such that to allow on-line design and implementation and, thus, yield a self-tuning control algorithm. The algorithm is implemented on a digital processor and its performance assessed in the cancellation of broadband noise in a free-field environment.

A flexible beam system in transverse vibration is considered for vibration suppression. Such a system has a large number of modes although in most cases the lower modes are the dominant ones requiring attention. The unwanted vibrations in the structure are assumed to be caused by a single point disturbance of broadband nature. These are detected and suitable suppression signals generated via point actuators to yield vibration suppression over a broad frequency range along the beam. The self-tuning control algorithm developed within the ANC system is used in a 'systems' context and implemented accordingly within an SIMO active vibration control (AVC) structure and its performance assessed in the vibration suppression of a flexible beam system.

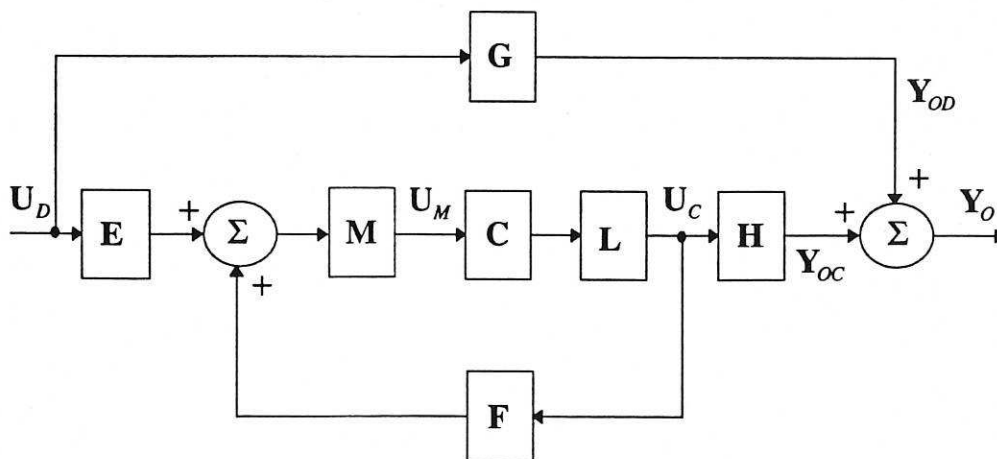
## 2 ACTIVE NOISE CONTROL

A schematic diagram of the geometric arrangement of an SIMO ANC structure is shown in Figure 1(a). The (unwanted) primary noise is detected by a detector (sensor), located at a distance  $r_e$  relative to the primary source and distance  $r_f$  relative to secondary (cancelling)

source  $i$  ( $i = 1, \dots, k$ ). The detected signal is processed by an SIMO controller of suitable frequency-dependent characteristics and fed to a set of  $k$  secondary sources. The secondary signals thus generated interfere with the primary noise so that to achieve a reduction in the level of the noise at and in the vicinity of observation points  $j$  ( $j = 1, \dots, k$ ), located at distances  $r_{gi}$  relative to the primary source and  $r_{hij}$  relative to secondary source  $i$ , in the medium.



(a)



(b)

Figure 1: Active noise control structure;  
 (a) Schematic diagram.  
 (b) Block diagram.

A frequency-domain equivalent block diagram of the ANC structure is shown in Figure 1(b), where,  $\mathbf{E} = [e]$  is a  $1 \times 1$  matrix representing the transfer characteristics of the path, through the distance  $r_e$ , between the primary source and the detector,  $\mathbf{F}$  is a  $k \times 1$  matrix representing the transfer characteristics of the paths, through the distances  $r_{fi}$  ( $i = 1, \dots, k$ ), from the secondary sources to the detection point,  $\mathbf{G}$  is a  $1 \times k$  matrix representing the transfer characteristics of the paths, through the distances  $r_{gj}$  ( $j = 1, \dots, k$ ), from the primary source to the observation points,  $\mathbf{H}$  is a  $k \times k$  matrix representing the transfer characteristics of the paths, through the distances  $r_{hij}$ , from the secondary sources to the observation points,  $\mathbf{M} = [m]$  is a  $1 \times 1$  matrix representing the transfer characteristics of the detector,  $\mathbf{L}$  is a  $k \times k$  diagonal matrix representing the transfer characteristics of the secondary sources and  $\mathbf{C}$  is a  $1 \times k$  matrix representing the transfer characteristics of the controller;

$$\begin{aligned} \mathbf{F} &= [f_1 \quad f_2 \quad \dots \quad f_k]^T \\ \mathbf{G} &= [g_1 \quad g_2 \quad \dots \quad g_k] \\ \mathbf{C} &= [c_1 \quad c_2 \quad \dots \quad c_k] \end{aligned}, \quad \mathbf{H} = \begin{bmatrix} h_{11} & h_{12} & \dots & h_{1k} \\ h_{21} & h_{22} & \dots & h_{2k} \\ \vdots & \vdots & \vdots & \vdots \\ h_{k1} & h_{k2} & \dots & h_{kk} \end{bmatrix}, \quad \mathbf{L} = \begin{bmatrix} l_1 & 0 & \dots & 0 \\ 0 & l_2 & \dots & 0 \\ \vdots & \vdots & \vdots & \vdots \\ 0 & 0 & \dots & l_k \end{bmatrix} \quad (1)$$

$\mathbf{U}_D$  is a  $1 \times 1$  matrix representing the disturbance (primary) signal at the source,  $\mathbf{Y}_{OD}$  is a  $1 \times k$  matrix representing the primary signal at the observation points,  $\mathbf{U}_C$  is a  $1 \times k$  matrix representing the control (secondary) signals at the source,  $\mathbf{Y}_{OC}$  is a  $1 \times k$  matrix representing the control signals at the observation points,  $\mathbf{U}_M$  is a  $1 \times 1$  matrix representing the detected signal and  $\mathbf{Y}_O$  is a  $1 \times k$  matrix representing the observed signals.

The block diagram in Figure 1(b) can be thought either in the continuous complex frequency,  $s$ , domain or in the discrete complex frequency,  $z$ , domain. The analysis and design presented in this report apply equally to both domains. The implementation of the controller, however, is carried out in the discrete-time domain.

The control structure in Figure 1 corresponds to the basic structure proposed by Lueg in his patent where the time delay is implemented by the physical separation between the primary and secondary sources (Lueg, 1936). A significant amount of consideration has subsequently been given to this structure in various applications. Conover, Hesselman and

Ross have employed this structure in the cancellation of transformer noise (Conover, 1956; Hesselman, 1978; Ross, 1978). Ross has considered the design, Roure has analysed the stability, Eriksson, et al. have considered the implementation of this structure in the cancellation of the one-dimensional duct noise (Eriksson *et al.*, 1987, 1988; Munjal and Eriksson, 1988; Ross, 1982; Roure, 1985). Nelson, et al. have analysed the performance of this structure in the cancellation of enclosed sound fields (Bullmore *et al.*, 1987; Elliott *et al.*, 1987a; Nelson *et al.*, 1987). Tokhi and Leitch have considered the design, stability, performance and implementation of this structure in the cancellation of noise in three-dimensional propagation (Leitch and Tokhi, 1986, 1987; Tokhi and Leitch, 1989, 1991a,b,c).

The objective in Figure 1 is to achieve full (optimum) cancellation at the observation points. This is equivalent to the minimum variance design criterion in a stochastic environment. This requires the primary and secondary signals at each observation point to be equal in amplitudes and have a phase difference of  $180^0$  relative to one another;

$$\mathbf{Y}_o = \mathbf{Y}_{OD} + \mathbf{Y}_{OC} = 0 \quad (2)$$

Using the block diagram of Figure 1(b) the signals  $\mathbf{Y}_{OD}$  and  $\mathbf{Y}_{OC}$  can be obtained as

$$\begin{aligned} \mathbf{Y}_{OD} &= \mathbf{U}_D \mathbf{G} \\ \mathbf{Y}_{OC} &= \mathbf{U}_D \mathbf{E} \mathbf{G} \mathbf{M} \mathbf{C} \mathbf{L} [\mathbf{I} - \mathbf{F} \mathbf{M} \mathbf{C} \mathbf{L}]^{-1} \mathbf{H} \end{aligned} \quad (3)$$

Where  $\mathbf{I}$  is the identity matrix. Substituting for  $\mathbf{Y}_{OD}$  and  $\mathbf{Y}_{OC}$  from equation (3) into equation (2) and solving for  $\mathbf{C}$  yields

$$\mathbf{C} = \mathbf{M}^{-1} [\mathbf{G} \mathbf{H}^{-1} \mathbf{F} - \mathbf{E}]^{-1} \mathbf{G} \mathbf{H}^{-1} \mathbf{L}^{-1} \quad (4)$$

This is the required controller transfer function for optimum cancellation of broadband noise at the observation points. The controller thus designed is assured to be causal by making the number of zeros in each path either equal to or less than the number of poles accordingly. Note that, for given secondary sources and detection sensor the characteristics of the required controller are determined by the geometric arrangement of system components. Among these, it is possible with some arrangements that the determinant

$|GH^{-1}F - E|$  will be zero or close to zero, requiring the controller to have impractically large gains. Moreover, with some geometrical arrangements of system components, the (positive) feedback loops due to the secondary signals reaching the detection point can cause the system to become unstable. Therefore, for the system performance to be robust, a consideration of the system in relation to the geometric arrangement of system components is important at a design stage (Tokhi, 1995; Tokhi and Leitch, 1991c).

The controller transfer function in equation (4) can be realised either as a fixed digital or analogue or hybrid (combined analogue and digital) controller through a process of measurement/estimation of the transfer characteristics of the propagation paths in the medium and through the sensor and actuators accordingly. In practice, the characteristics of sources of disturbance vary due to operating conditions, for instance, leading to time-varying spectra. Moreover, the characteristics of transducers, sensors and other electronic equipment used in the ANC system are subject to variation due to environmental effects, ageing, etc. Under such situations the system employing a fixed controller will not perform to a desired level. Thus, an ANC system is, in general, required to be capable of updating the controller characteristics in accordance with the changes in the system so that the required level of performance is achieved and maintained. To do this a self-tuning control strategy, allowing on-line design and implementation of the controller, can be utilised.

## **2.1 Self-tuning active noise control**

The design relation given for the controller transfer function in equation (4) is in a form that is not suitable for on-line implementation. To allow on-line design and implementation of the controller, equivalent design rules based on on-line measurement of (input/output) signals of the system are required. To devise such a strategy, a self-tuning control mechanism is developed.

Self-tuning control is distinguished as a class of adaptive control mechanisms (Harris and Billings, 1981; Tokhi and Leitch, 1992; Wellstead and Zarrop, 1991). It essentially consists of the processes of identification and control, both implemented on-line. The identification process is mainly concerned with on-line modelling of the plant to be

controlled and, thus, incorporates a suitable system identification algorithm. The control process, on the other hand, is concerned with the design and implementation of the controller using the plant model and, thus, incorporates a suitable controller design criterion. In this manner, various types of self-tuning control algorithm can be designed depending on the type of the identification algorithm and controller design strategy employed. A self-tuning control algorithm can either be designed as an explicit combination of identification of a plant model and controller design or as an implicit algorithm in which the controller is identified directly (bypassing identification of the plant model). In this report an explicit self-tuning ANC algorithm, incorporating a recursive least squares (RLS) parameter estimation algorithm and the minimum variance design criterion, is developed.

To develop a self-tuning ANC system, consider Figure 1 with measurable input and output signals as the detected signal  $U_M$  and the observed signal  $Y_O$  respectively. Thus, owing to the state of each secondary source, a model of the system between the detection point and each observation point can be obtained. This will result in a set of models with equivalent transfer functions denoted by  $q_{oj}$  ( $j = 1, \dots, k$ ) when all the secondary sources are *off* and a further set of models with equivalent transfer functions denoted by  $q_{ij}$  when all the secondary sources are off except secondary source  $i$ . In this manner, a total of  $k(k+1)$  models can be constructed.

Using the block diagram in Figure 1(b), the detected signal  $U_M$  and the observed signal  $Y_O$  can be obtained as

$$\begin{aligned} U_M &= U_D \mathbf{EM}(\mathbf{I} - \mathbf{CLFM})^{-1} \\ Y_O &= U_D \{ \mathbf{G} + \mathbf{EMCL}(\mathbf{I} - \mathbf{FMCL})^{-1} \mathbf{H} \} \end{aligned} \quad (5)$$

Thus, the equivalent transfer functions of system's models, for the corresponding situation under consideration, is given by the ratio  $Y_O U_M^{-1}$  in equation (5).

Substituting for  $E$ ,  $F$ ,  $G$ ,  $H$ ,  $L$  and  $C$  from equation (1) into equation (4) and simplifying yields a relation for each element of  $C$  as

$$c_i = \frac{1}{b_i} \frac{\sum_{j=1}^k g_j H_{ij}}{\sum_{i=1}^k f_i \left( \sum_{j=1}^k g_j H_{ij} \right) - e|\mathbf{H}|}; \quad i = 1, \dots, k \quad (6)$$

where  $c_i$  is the  $i$ th element of  $\mathbf{C}$ ,  $b_i = \mathbf{M}l_i = ml_i$  with  $l_i$  representing the transfer characteristics of secondary source  $i$ ,  $g_j$  represents the transfer characteristics of the path, through the distance  $r_{gj}$ , between the primary source and observation point  $j$ ,

$$H_{ij} = (-1)^{i+j} \begin{vmatrix} h_{11} & h_{12} & \cdots & h_{1(j-1)} & h_{1(j+1)} & \cdots & h_{1k} \\ h_{21} & h_{22} & \cdots & h_{2(j-1)} & h_{2(j+1)} & \cdots & h_{2k} \\ \vdots & \vdots & \vdots & \vdots & \vdots & \vdots & \vdots \\ h_{(i-1)1} & h_{(i-1)2} & \cdots & h_{(i-1)(j-1)} & h_{(i-1)(j+1)} & \cdots & h_{(i-1)k} \\ h_{(i+1)1} & h_{(i+1)2} & \cdots & h_{(i+1)(j-1)} & h_{(i+1)(j+1)} & \cdots & h_{(i+1)k} \\ \vdots & \vdots & \vdots & \vdots & \vdots & \cdots & \vdots \\ h_{k1} & h_{k2} & \cdots & h_{k(j-1)} & h_{k(j+1)} & \cdots & h_{kk} \end{vmatrix}$$

with  $h_{ij}$  representing the transfer characteristics of the path, through the distance  $r_{hij}$ , between secondary source  $i$  and observation point  $j$  and  $|\mathbf{H}|$  represents the determinant of the matrix  $\mathbf{H}$ .

To obtain  $c_i$  in equation (6) in terms of the transfer functions of system models, two cases, namely, when all secondary sources are *off* and when only secondary source  $i$  is *on*, are considered (the primary source is *on* throughout).

To switch *off* all secondary sources the 'controller' in Figure 1(a) is replaced with an 'open' switch. This in terms of the block diagram in Figure 1(b) is equivalent to all entries in  $\mathbf{C}$  initialised to zero;

$$\mathbf{C} = [0 \quad 0 \quad \cdots \quad 0] \quad (7)$$

Substituting for  $\mathbf{C}$  from equation (7) into equation (5) and simplifying yields the equivalent transfer functions  $q_{oj}$  ( $j = 1, \dots, k$ ) as

$$q_{oj} = \frac{g_i}{me}; \quad j = 1, \dots, k \quad (8)$$

To keep only secondary source  $i$  on the 'controller' in Figure 1(a) is replaced by a switch in which only the path through to secondary source  $i$  is closed. This in terms of the block diagram in Figure 1(b) is equivalent to the matrix  $C$  initialised to unity at location  $i$  and to zero in all other locations;

$$C = [0 \quad \dots \quad 0 \quad 1 \quad 0 \quad \dots \quad 0] \quad (9)$$

Note in equation (9) that, for simplicity purposes, element  $i$  of the controller is initialised to unity in this case. The procedure given below equally applies to the general situation where the path from the detector to secondary source  $i$  is closed through an electronic component of a particular transfer function. In this case, element  $i$  of the controller in equation (9) can be replaced by this (initial) transfer function and thus carried throughout the synthesis process. It must be noted, however, that this initial transfer function should be included within the ANC system in cascade with the required controller transfer function during the implementation process. Note that the feedback loop formed through secondary source  $i$  to the detector by switching on the corresponding controller path may cause the system to become unstable. Under such a situation the choice of utilising an initial transfer function instead of the switch may be favoured to bring the loop gain below unity and thus allow the system to be stable during the identification phase.

Substituting for  $C$  from equation (9) into equation (5), simplifying and using equation (8) yields

$$q_{ij} = q_{oj} \left[ \left( \frac{h_{ij}e}{g_j} - f_i \right) b_i + 1 \right]$$

or

$$\left( \frac{h_{ij}e}{g_j} - f_i \right) b_i = \frac{q_{ij}}{q_{oj}} - 1; \quad i = 1, \dots, k \quad \text{and} \quad j = 1, \dots, k \quad (10)$$

Adding the relations for  $i = 1$  to  $k$  in equation (10) yields

$$\sum_{i=1}^k \left( \frac{h_{ij} e}{g_j} - f_i \right) b_i = \frac{1}{q_{oj}} \sum_{i=1}^k q_{ij} - k; \quad j = 1, \dots, k \quad (11)$$

Equation (11) corresponds to the system description in Figure 1 when all the secondary sources are switched on; i.e. all entries in the matrix  $C$  initialised to unity. Solving this equation for  $b_i$  ( $i = 1, \dots, k$ ), manipulating each and using equation (6) yields

$$\frac{1}{c_i} = 1 - \frac{1}{W_i} \left\{ \sum_{j=1}^k \frac{g_j V_{ij}}{q_{oj}} \left( \sum_{p=1}^k q_{pj} - k + 1 \right) \right\}; \quad i = 1, \dots, k \quad (12)$$

where,

$$V_{ij} = (-1)^{i+j} \begin{vmatrix} e & f_1 & \cdots & f_{(i-1)} & f_{(i+1)} & \cdots & f_k \\ g_i & h_{11} & \cdots & h_{(i-1)1} & h_{(i+1)1} & \cdots & h_{k1} \\ \vdots & \vdots & \vdots & \vdots & \vdots & \vdots & \vdots \\ g_{j-1} & h_{1(j-1)} & \cdots & h_{(i-1)(j-1)} & h_{(i+1)(j-1)} & \cdots & h_{k(j-1)} \\ g_{j+1} & h_{1(j+1)} & \cdots & h_{(i-1)(j+1)} & h_{(i+1)(j+1)} & \cdots & h_{k(j+1)} \\ \vdots & \vdots & \vdots & \vdots & \vdots & \vdots & \vdots \\ g_k & h_{1k} & \cdots & h_{(i-1)k} & h_{(i+1)k} & \cdots & h_{kk} \end{vmatrix}$$

$$W_i = \sum_{j=1}^k g_j V_{ij}$$

Simplifying equation (12) and using equations (10) and (11) yields

$$c_i = Q_i \left[ \sum_{p=0}^k Q_p \right]^{-1}; \quad i = 1, \dots, k \quad (13)$$

where,

$$Q_o = \begin{vmatrix} q_{11} & q_{12} & \cdots & q_{1k} \\ q_{21} & q_{22} & \cdots & q_{2k} \\ \vdots & \vdots & \vdots & \vdots \\ q_{k1} & q_{k2} & \cdots & q_{kk} \end{vmatrix}, \quad Q_i = (-1)^i \begin{vmatrix} q_{01} & q_{02} & \cdots & q_{0k} \\ q_{11} & q_{12} & \cdots & q_{1k} \\ \vdots & \vdots & \vdots & \vdots \\ q_{(i-1)1} & q_{(i-1)2} & \cdots & q_{(i-1)k} \\ q_{(i+1)1} & q_{(i+1)2} & \cdots & q_{(i+1)k} \\ \vdots & \vdots & \vdots & \vdots \\ q_{k1} & q_{k2} & \cdots & q_{kk} \end{vmatrix}$$

Equation (13) gives the required controller design rules in terms of the transfer characteristics  $q_{oj}$  and  $q_{ij}$  ( $i = 1, \dots, k ; j = 1, \dots, k$ ) of system models. The controller can thus be designed on-line by first estimating  $q_{oj}$  and  $q_{ij}$  using a suitable system identification algorithm and then using equation (13) to design the controller. The controller designed in this manner can easily be implemented on a digital processor and the required control signals generated and applied in real-time. Moreover, to achieved on-line adaptation of the controller characteristics whenever a change in the system is sensed, a supervisory level control is required. The supervisor can be designed to monitor system performance and, based on a pre-specified quantitative measure of cancellation, initiate self-tuning control accordingly. In this manner, the actual cancellation achieved at the observation point can be measured, if this is within the pre-specified range then the controller will continue to process the detected signal, generate and output the cancelling signals. If the cancellation, however, is outside the specified limit then self-tuning will be initiated at the identification level. The self-tuning ANC algorithm can be outlined on the basis of the above as follows

- (1) Switch off all secondary sources, estimate transfer functions  $q_{oj}$  ( $j = 1, \dots, k$ ).
- (2) Switch on secondary source  $i$  ( $i = 1, \dots, k$ ), estimate transfer functions  $q_{ij}$  ( $j = 1, \dots, k$ ).
- (3) Use equation (13) to obtain the transfer function of the controller  $c_i$  ( $i = 1, \dots, k$ ).
- (4) Implement the controller, to generate the control signals.
- (5) Measure system performance and compare with pre-specified index, if within specified range then go to (4) otherwise go to (1).

The self-tuning ANC control system implemented according to the above algorithm is described in Figure 2, where 'plant' denotes the system in Figure 1 with the detected signal as the input and the observed signals as the outputs.

The transfer functions  $q_{oj}$  and  $q_{ij}$  are represented in the discrete complex frequency domain. Such a formulation also allows the corresponding time-domain representations of the system models in the form of difference equations. The RLS algorithm used in the

above utilises the difference equation representations with specified orders and, upon measurement of input/output signals of the system, produces parameters of the system model (Tokhi and Leitch, 1992). These parameters are used in steps (1) and (2) above to obtain the corresponding transfer function representations of the models,  $q_{oj}$  and  $q_{ij}$ . The estimated transfer functions  $q_{oj}$  and  $q_{ij}$  thus obtained are used in equation (13) to obtain the required controller transfer functions  $c_i$ . These are then implemented in step (4) above in the time domain using the corresponding difference equation representations.

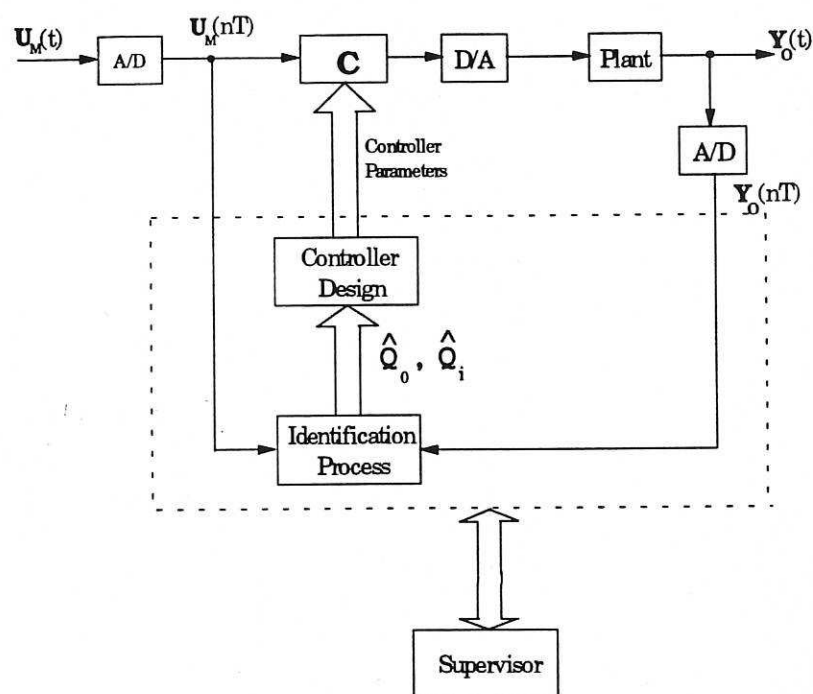


Figure 2: Self-tuning active controller.

In implementing the self-tuning control algorithm described above, several issues of practical importance need to be given careful consideration. These include properties of the disturbance signal, robustness of the estimation and control, system stability and processor-related issues such as wordlength, speed and computational power.

In simulation experiments where the primary signal can be chosen properly to satisfy the robustness requirements of the control algorithm the problems due to the properties of the input signal will not arise. In practice, however, where the disturbance force may also excite those dynamics of the system which are not of interest, care must be taken to

condition the input signal properly before sampling. Robustness of the control algorithm is related to the accuracy of the estimated plant model. This in turn depends on properties of the input signal, proper initialisation of the parameter estimation algorithm, model order and accuracy of computation (Tokhi and Leitch, 1991b). The computational accuracy is related to the processor's dynamic range of computation, determined by the processor wordlength and type of arithmetic. With a processor supporting fixed-point arithmetic for example it is important to take necessary precautions against problems due to overflow and inaccuracies due to truncation/rounding of variables (Tokhi and Leitch, 1991b).

In employing the minimum variance design criterion, a problem commonly encountered is that of instability of system, specially, when non-minimum phase models are involved. Note in the controller design rules, equation (13), that such a situation will result in a non-minimum phase and unstable controller with the unstable poles approximately cancelling the corresponding zeros that are outside the stability region. Thus, to avoid this problem of instability either the estimated models can be made minimum-phase by reflecting their non-invertible zeros into the stability region and using the resulting minimum-phase models to design the controller or once the controller is designed the poles and zeros that are outside the stability region can be reflected into the stability region. In this manner, a factor  $(1 - pz^{-1})$  corresponding to a pole/zero at  $z = p$ , in the complex  $z$ -plane, that is outside the stability region can be reflected into the stability region by replacing the factor with  $(p - z^{-1})$ .

The supervisory level control described above is used as a performance monitor. In addition to monitoring system performance, it can also be facilitated with further levels of intelligence, for example, monitoring system stability and avoiding problems due to non-minimum phase models as describe above, verifying controller characteristics on the basis of practical realisation to make sure that impractically large controller gains are not required as discussed earlier, system behaviour in a transient period, model structure validation etc.

## 2.2 Simulation algorithm

To allow development of a suitable simulation environment for test and verification of the control strategy, consider a loudspeaker, with its drive amplifier, and a microphone incorporating its pre-amplifier, located at a set distance  $r_m$  in front of the loudspeaker. This is shown in an equivalent block diagram in Figure 3 where,  $l$  represents the transfer characteristics of the loudspeaker,  $m$  represents the transfer characteristics of the microphone,  $(A/r_m)\exp(-jr_m\omega/c)$  is the transfer characteristics of the acoustic path through  $r_m$  with  $A$  as a constant,  $c$  as speed of sound and  $\omega$  the radian frequency. Note that the acoustic medium is assumed to be non-dispersive. Let the amplitude and phase response of the system in Figure 3 from the input of the loudspeaker to the output of the microphone as a function of the frequency  $\omega$  be denoted by  $A_m$  and  $Q_m$  respectively;

$$A_m \exp(jQ_m) = ml \frac{A}{r_m} \exp(-jr_m\omega/c) \quad (14)$$

The frequency response of the acoustic paths through  $r_e$ ,  $r_{fi}$ ,  $r_{gj}$  and  $r_{hij}$  ( $i = 1, \dots, k$ ;  $j = 1, \dots, k$ ) in Figure 1 can be written as

$$\begin{aligned} e(j\omega) &= (A/r_e)\exp(-jr_e\omega/c) \\ f_i(j\omega) &= (A/r_{fi})\exp(-jr_{fi}\omega/c) \\ g_j(j\omega) &= (A/r_{gj})\exp(-jr_{gj}\omega/c) \\ h_{ij}(j\omega) &= (A/r_{hij})\exp(-jr_{hij}\omega/c) \end{aligned} \quad (15)$$

Assuming  $l_1 = \dots = l_k = l$  in equation (1), let  $E'$ ,  $F'$ ,  $G'$  and  $H'$  be transfer characteristics defined as

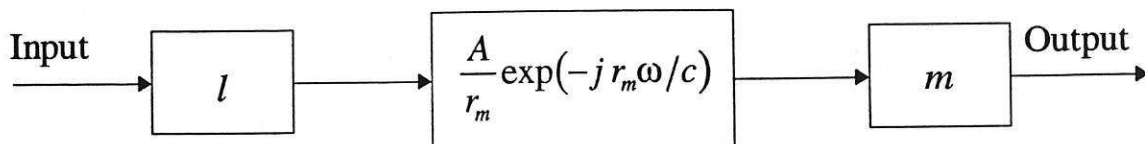


Figure 3: Frequency response measurement.

$$\begin{aligned}
\mathbf{E}' &= m\mathbf{E} = \{A_e \exp(jQ_e)\} \\
\mathbf{F}' &= m\mathbf{F} = \{A_{f_i} \exp(jQ_{f_i})\} \\
\mathbf{G}' &= m\mathbf{G} = \{A_{g_j} \exp(jQ_{g_j})\} \\
\mathbf{H}' &= m\mathbf{H} = \{A_{h_{ij}} \exp(jQ_{h_{ij}})\}
\end{aligned} \tag{16}$$

Using equations (14), (15) and (16) yields

$$\begin{aligned}
A_e &= A_m (r_m/r_e) \quad , \quad Q_e = Q_m - (r_e - r_m)\omega/c \\
A_{f_i} &= A_m (r_m/r_{f_i}) \quad , \quad Q_{f_i} = Q_m - (r_{f_i} - r_m)\omega/c \\
A_{g_j} &= A_m (r_m/r_{g_j}) \quad , \quad Q_{g_j} = Q_m - (r_{g_j} - r_m)\omega/c \\
A_{h_{ij}} &= A_m (r_m/r_{h_{ij}}) \quad , \quad Q_{h_{ij}} = Q_m - (r_{h_{ij}} - r_m)\omega/c
\end{aligned} \tag{17}$$

Using equation (16), the controller design relation in equation (4) can equivalently be expressed as

$$\mathbf{C} = [\mathbf{G}'\mathbf{H}'^{-1}\mathbf{F}' - \mathbf{E}']^{-1} \mathbf{G}'\mathbf{H}'^{-1}$$

Thus, with given data for  $A_m$  and  $Q_m$  a suitable simulation environment characterising the system in Figure 1 can be constructed by obtaining the frequency responses  $\mathbf{E}'$ ,  $\mathbf{F}'$ ,  $\mathbf{G}'$  and  $\mathbf{H}'$  with specified arrangements of the primary source, secondary sources, detector and observers using the corresponding values for  $r_e$ ,  $r_{f_i}$ ,  $r_{g_j}$  and  $r_{h_{ij}}$  and equation (17).

This results in an equivalent block diagram of the ANC system as shown in Figure 4. Note that the arrangement in Figure 4 assumes that the primary signal is also provided through a loudspeaker of the characteristics in Figure 3 with which the generality of the noise characteristics is not lost. Signal propagation through the system in Figure 1 can thus be simulated using the block diagram in Figure 4 either in the frequency domain or in the time-domain.

### 2.3 Implementation and results

To implement the ANC simulation algorithm, an experiment was conducted using the arrangement shown in Figure 3 with  $r_m = 0.03$  metres. A sine wave of fixed amplitude and phase was fed into the power amplifier and the frequency varied over the range 0 – 500 Hz. The amplitude and phase of the microphone output was measured relative to the input

and recorded to enable the gain and phase of the system be obtained. The amplitude and phase characteristics of the system thus measured are shown in Figure 5. These were used to realise and implement the simulation environment as outlined above. The algorithm was coded using MATLAB and implemented on a SUN workstation. The self-tuning ANC system was implemented within this environment with a pseudo-random binary sequence (PRBS), simulating a broadband signal in the range 0–512 Hz as the primary noise source. The dynamic range of the simulation environment was extended by interpolating the corresponding measured data so that to match the frequency range of the primary signal.

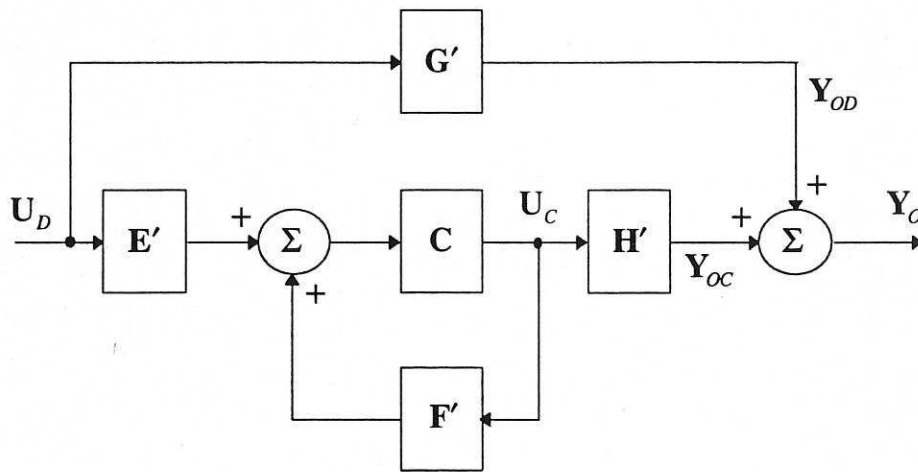
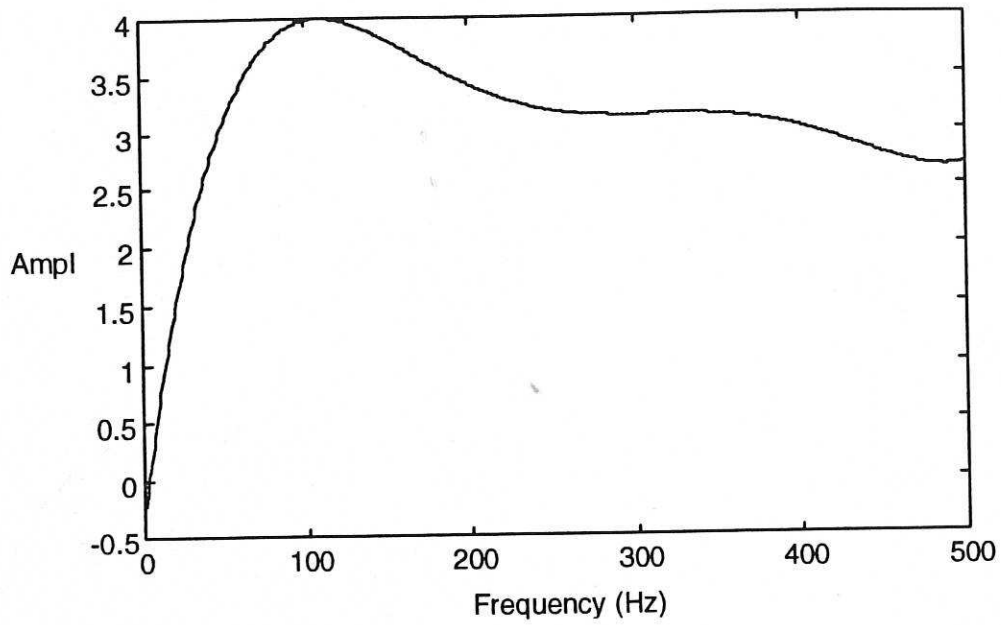
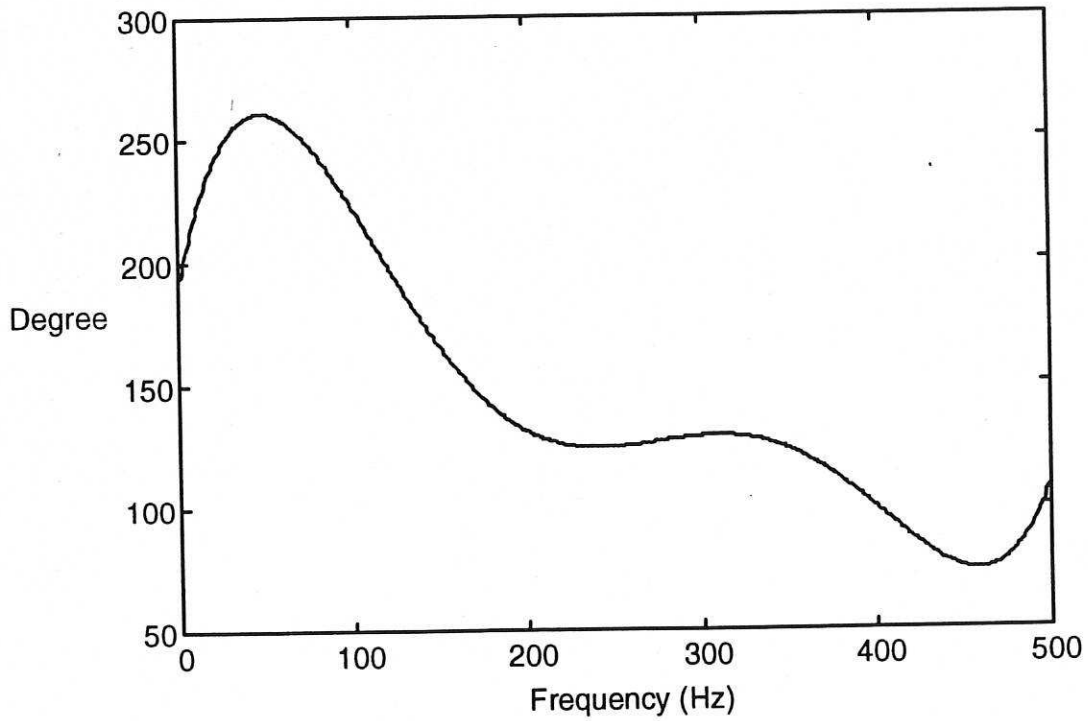


Figure 4: Block diagram of the simulated feedforward ANC structure.

The system was first realised within a single-input single-output (SISO) structure with second order models for  $q_{01}$  and  $q_{11}$ . The autopower spectral density of the noise was obtained at the observation point before and after cancellation and their difference giving the cancelled spectrum was evaluated. The performance of the system thus obtained is shown in Figure 6. As noted, an average cancellation level of about 20 dB was achieved over the broad frequency range of 0-512 Hz. Note that the cancellation at frequencies below 25 Hz is lower and decreases with frequency, resulting reinforcement below 20 Hz. This, as noted in Figure 5, is due to the corresponding large signal attenuation occurring in the loudspeaker within this frequency region.



(a)



(b)

Figure 5: Transfer characteristics of loudspeaker-microphone combination;  
(a) System gain.  
(b) System phase.

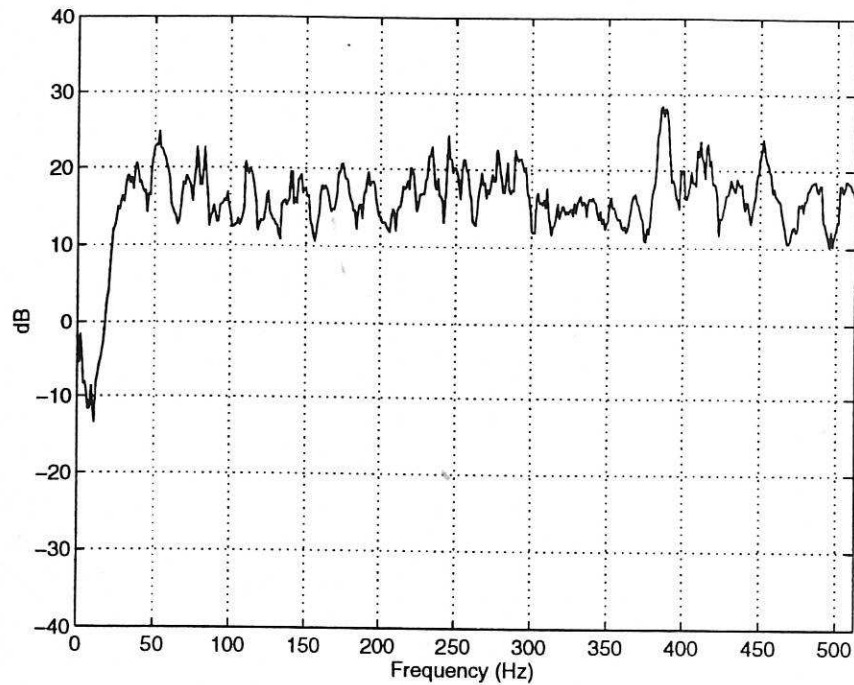
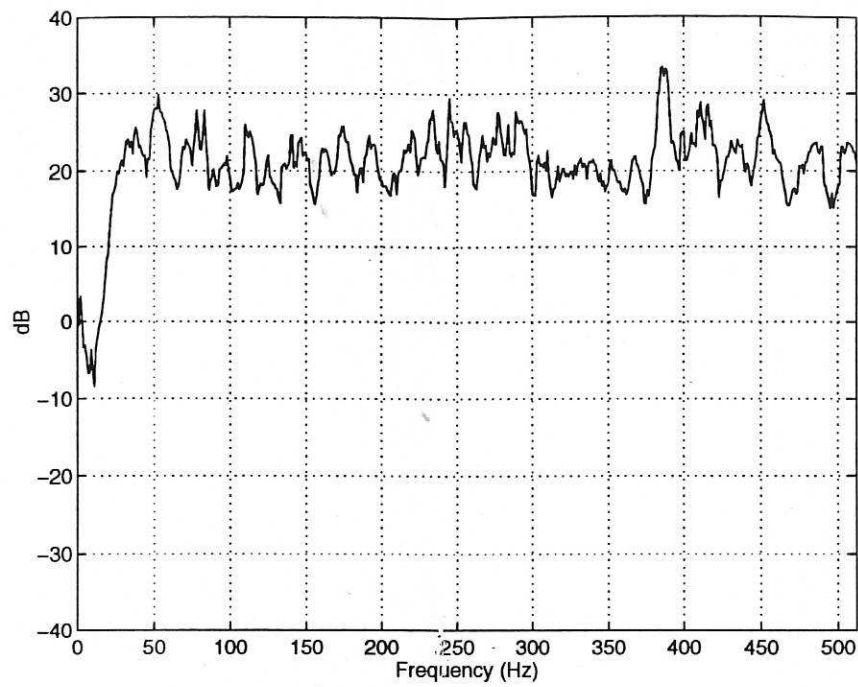


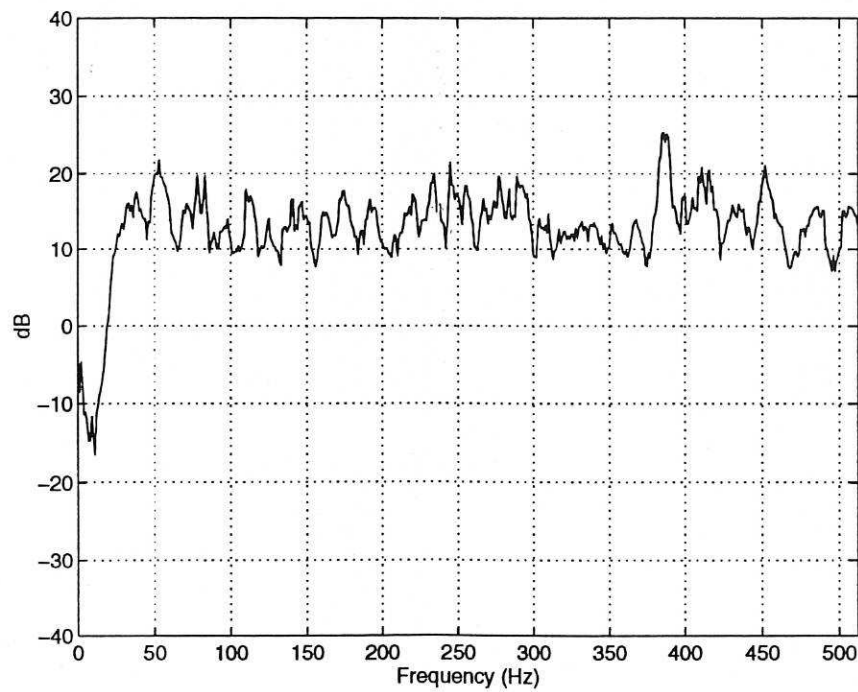
Figure 6: Cancelled spectrum at the observation point with the SISO self-tuning ANC system.

To investigate the performance of the self-tuning active control algorithm with multiple secondary sources, the system was realised within an SIMO structure incorporating two secondary sources and its performance monitored at the observation points. Figure 7 shows the performance of the system under this situation. As noted, an average cancellation level of above 20 dB was achieved at each observation point over the broad frequency range of the noise. A similar trend in the level of cancellation for frequencies below 25 Hz is seen as noted with the SISO system due to the loudspeaker characteristics.

It is noted in Figures 6 and 7 that the self-tuning active control algorithm has performed to a significant level in the cancellation of broadband noise using second order system models. It is possible to enhance the performance of the system further by increasing the orders of the system models. The consequences of this would be an increase in the number of parameters to be identified at the identification stage and an increase in the total execution time of the algorithm, affecting the real-time requirements of the system. However, these problems can be overcome by employing more powerful computing platforms.



(a)



(b)

Figure 7: Cancelled spectrum with the SIMO self-tuning ANC system;  
(a) Observation point 1.  
(b) Observation point 2.

### 3 ACTIVE VIBRATION CONTROL

Active vibration control is realised in a similar manner as active noise control. The design of an AVC system depends upon the complexity of the structure under consideration and the nature of the disturbance process. A flexible beam system in transverse vibration is considered here. Such a system has an infinite number of modes although in most cases the lower modes are the dominant ones requiring attention.

A schematic diagram of the AVC system is shown in Figure 8. The unwanted vibrations in the structure are assumed to be due to a single (primary) point disturbance force of broadband nature. These are detected by a point detector, processed by a controller to generate suitable (secondary) suppression signals via point actuator(s) so that to yield vibration suppression over a broad frequency range at observation point(s) along the beam. A frequency-domain equivalent block diagram of the AVC system in Figure 8 will give rise to that of the ANC system in Figure 1(b), with a similar interpretation of the transfer functions and signals involved. In this manner, the required controller transfer functions for optimum vibration suppression at the observation points is, therefore, given as in equation (2) with the corresponding equivalent relation suitable for on-line design and implementation as in equation (13). Therefore, a similar formulation of the self-tuning control algorithm developed for noise cancellation applies to vibration suppression in Figure 8, yielding a self-tuning AVC algorithm. To meet the observability and controllability requirements, the system components in Figure 8 are suitably placed relative to one another. For the disturbance signal to be measured properly, for instance, the detector is required to be placed close to the primary source and such that to detect the dynamic modes of interest of the system. Moreover, to achieve vibration suppression over a broad range of frequencies, the actuator should be located such that to excite all the dynamic modes of interest of the beam. Integral to these requirements is, additionally, to ensure that the arrangement results in a practically realisable controller and stable system, as discussed earlier within ANC.

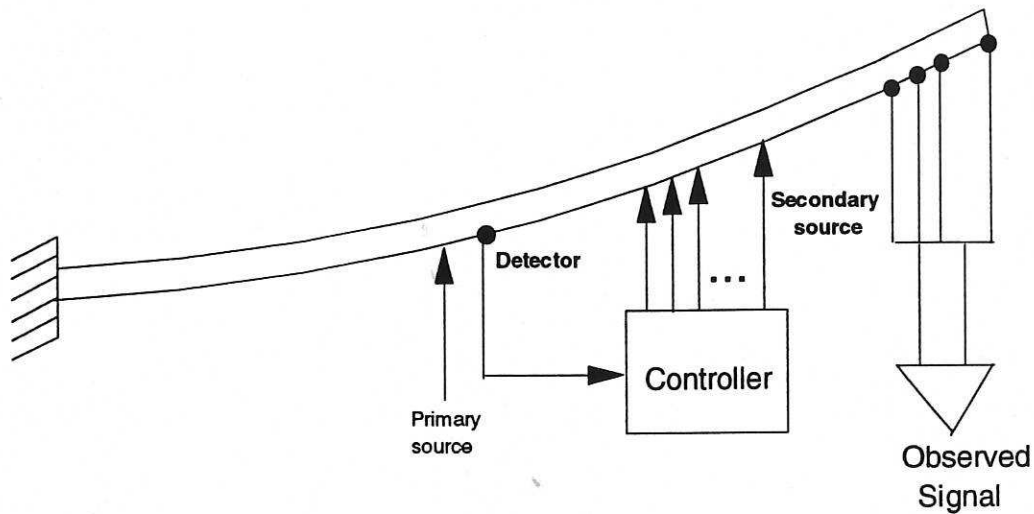


Figure 8: Active vibration control structure.

### 3.1 Simulation algorithm

Consider a flexible beam of length  $l$ , fixed at both ends, with a force  $U(x, t)$  applied at a distance  $x$  from one end of the beam at time  $t$ . This will result in a deflection,  $y(x, t)$ , of the beam from its stationary (unmoved) position at the point where the force has been applied. The motion of the beam in transverse vibration is governed by the well known fourth-order partial differential equation (PDE) (Virk and Kourmoulis, 1988)

$$\mu^2 \frac{\partial^4 y(x, t)}{\partial x^4} + \frac{\partial^2 y(x, t)}{\partial t^2} = \frac{1}{m} U(x, t) \quad (18)$$

where  $\mu$  is a beam constant given by  $\mu^2 = EI/\rho A$ , with  $\rho$ ,  $A$ ,  $I$  and  $E$  representing the mass density, cross-sectional area, moment of inertia of the beam and the Young's modulus respectively, and  $m$  is the mass of the beam. The corresponding boundary conditions at the two ends of the beam are given by

$$\begin{aligned} y(0, t) = 0 \quad \text{and} \quad \frac{\partial y(0, t)}{\partial x} = 0 \\ y(l, t) = 0 \quad \text{and} \quad \frac{\partial y(l, t)}{\partial x} = 0 \end{aligned} \quad (19)$$

To obtain a solution to the PDE, describing the beam motion, the partial derivative terms in equation (18) and the boundary conditions in equation (19) are approximated using first order central finite difference approximations. This involves a discretisation of

the beam into a finite number of equal-length sections (segments), each of length  $\Delta x$ , and considering the beam motion (deflection) for the end of each section (grid-point) at equally-spaced time steps of duration  $\Delta t$ . In this manner, dividing the beam into  $n-1$  sections ( $n$  grid-points), equations (18) and (19) can be represented in discrete form as

$$\begin{aligned} Y_{j+1} &= -Y_{j-1} - \lambda^2 S Y_j + (\Delta t)^2 U(x, t) \frac{1}{m} \\ y_{0,j} &= 0 \quad \text{and} \quad y_{-1,j} = y_{1,j} \\ y_{n,j} &= 0 \quad \text{and} \quad y_{n+1,j} = y_{n-1,j} \end{aligned} \quad (20)$$

where,  $\lambda^2 = \mu^2 (\Delta t)^2 / (\Delta x)^4$ ,  $Y_k$  represents the deflection of the beam at time step  $k$ ;

$$Y_{j+1} = \begin{bmatrix} y_{1,j+1} \\ y_{2,j+1} \\ \vdots \\ y_{n,j+1} \end{bmatrix}, \quad Y_j = \begin{bmatrix} y_{1,j} \\ y_{2,j} \\ \vdots \\ y_{n,j} \end{bmatrix}, \quad Y_{j-1} = \begin{bmatrix} y_{1,j-1} \\ y_{2,j-1} \\ \vdots \\ y_{n,j-1} \end{bmatrix},$$

and  $S$  is a stiffness matrix, given (for  $n = 20$ , say) as

$$S = \begin{bmatrix} a & -4 & 1 & 0 & 0 & 0 & \cdots & \cdots & 0 \\ -4 & b & -4 & 1 & 0 & 0 & \cdots & \cdots & 0 \\ 1 & -4 & b & -4 & 1 & 0 & \cdots & \cdots & 0 \\ 0 & 1 & -4 & b & -4 & 1 & \cdots & \cdots & 0 \\ \cdots & \cdots \\ \cdots & \cdots \\ \cdots & \cdots & \cdots & \cdots & 1 & -4 & b & -4 & 1 \\ \cdots & \cdots & \cdots & \cdots & 0 & 1 & -4 & b & -4 \\ \cdots & \cdots & \cdots & \cdots & 0 & 0 & 1 & -4 & a \end{bmatrix}$$

with  $a = 7 - 7\lambda^{-2}$  and  $b = 6 - 2\lambda^{-2}$ . Equation (20) is the required relation for the simulation algorithm, characterising the behaviour of the flexible beam system, which can be implemented on a digital processor easily.

### 3.2 Implementation and results

In these simulation studies an aluminium type cantilever beam of length  $l = 0.635$  m,  $m = 0.03745$  kg and  $\mu = 1.3511$  was considered. Investigations were carried out to

determine a suitable number of segments the beam be divided into so that an adequate level of accuracy is achieved by the simulation algorithm in representing the characteristic behaviour of the beam. It was found through these investigations that reasonable accuracy will be achieved by dividing the beam into 20 equal-length segments. Thus, the beam was divided into 20 segments (21 grid-points) and to insure stability of the simulation algorithm a time discretisation step of 0.3 msec was used. To investigate the performance of the self-tuning active control algorithm in broadband vibration suppression, the beam simulation algorithm, as a test and verification platform, was implemented on a digital computer. To assess the performance of the algorithm a fixed (finite-duration) disturbance was used as the unwanted primary signal. While the frequency range of excitation used was 0-3000 Hz, analysis of the performance of the system was focused to 0-800 Hz which covers a large number of resonance modes of the beam and gives a sufficiently clear insight into its behaviour.

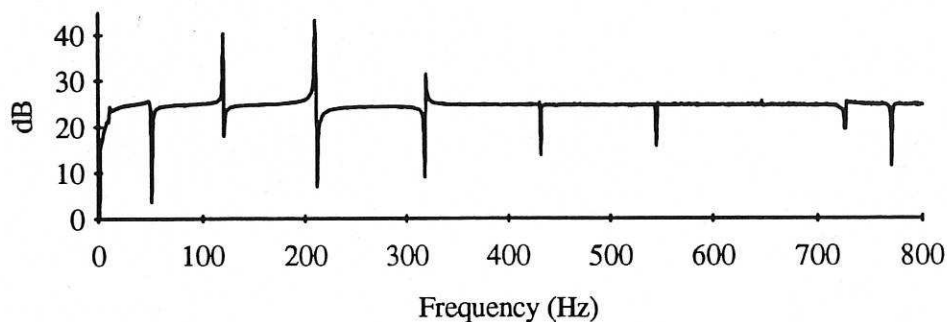


Figure 9: Cancelled spectrum with the SISO self-tuning AVC system at the observation point.

The self-tuning algorithm was first realised within an SISO structure with the primary and secondary sources located at grid points 11 and 10 respectively, the detector at grid-point 11 and the observer at grid-point 9 along the beam. Figure 9 shows the performance of the system, at the observation point, as the difference between the spectra before and after cancellation, i.e. the attenuated spectrum. It is noted that, on average, about 25 dB cancellation has been achieved over a broad range of frequencies of the disturbance covering most of the dominant modes of vibration. The sharp dips noted in Figure 9

correspond to the resonance modes of vibration of the beam. It is evidenced in the corresponding description given in terms of the average signal power throughout the length of the beam in Figure 10 that, the level of the unwanted disturbance has significantly been reduced throughout the length of the beam.

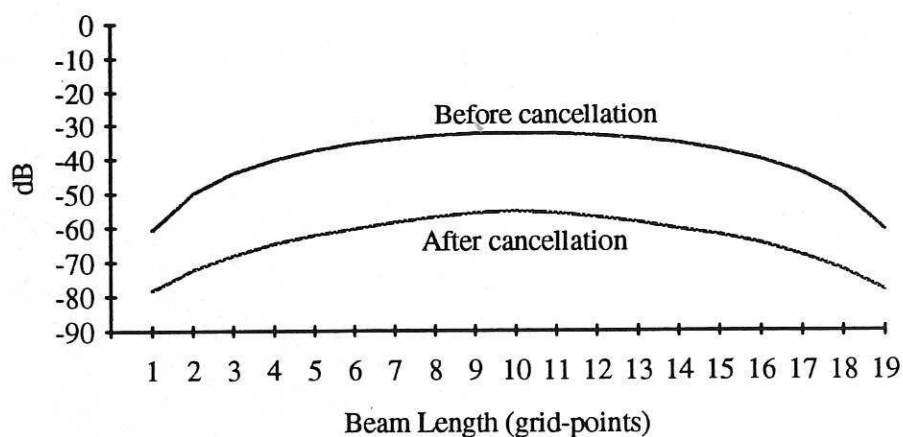
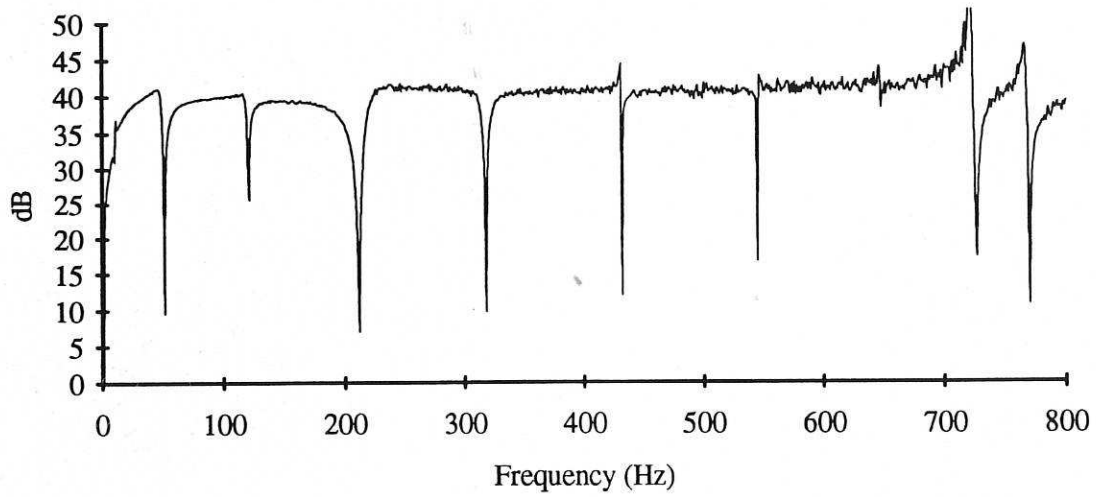
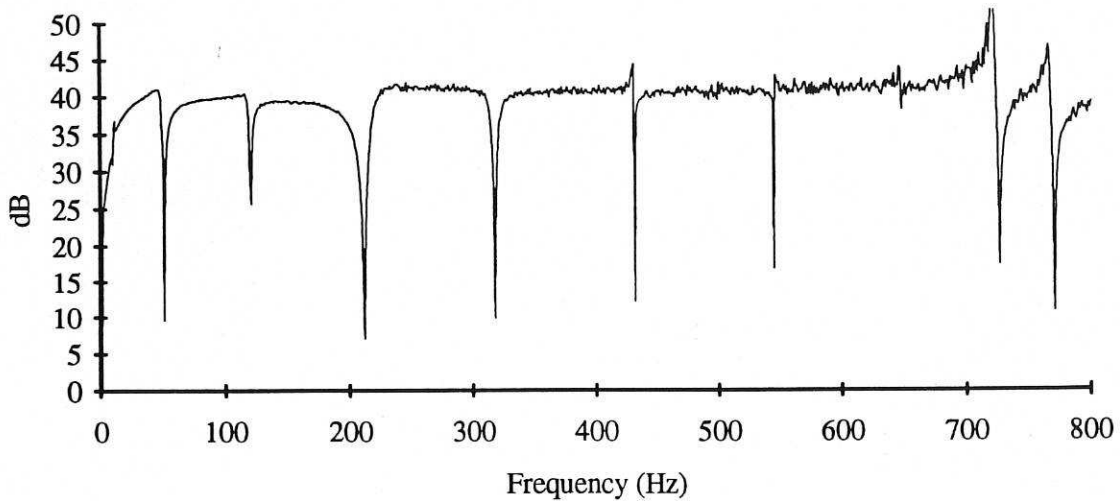


Figure 10: Average autopower spectral densities along the beam before and after cancellation with the SISO self-tuning AVC system.

To investigate the performance of the self-tuning AVC algorithm within an SIMO structure, a system with two secondary sources located at grid points 10 and 12, was realised. With the primary source and the detector both located at grid point 11, the self-tuning AVC system was implemented to achieve optimum cancellation at grid points 9 (observation point 1) and 13 (observation point 2). Figure 11 shows the performance of the system at the two observation points using a fixed disturbance force as the primary signal. It is seen that an average level of cancellation, over the broad frequency range of the disturbance, of at least 40 dB has been achieved at each observation point. The sharp dips, noted earlier with the SISO system as well, occur at the resonance frequencies of vibration of the beam. As compared with the performance of the SISO system in Figure 9, the amount of cancellation achieved at almost all the resonance modes is significantly larger with the SIMO system. Such a significant reduction in the level of the disturbance is reflected throughout the beam length as shown by the corresponding frequency-domain description of the beam behaviour before and after cancellation in Figure 12.



(a)



(b)

Figure 11: Attenuated spectrum of the disturbance with the SIMO self-tuning AVC system;  
(a) At observation point 1.  
(b) At observation point 2.

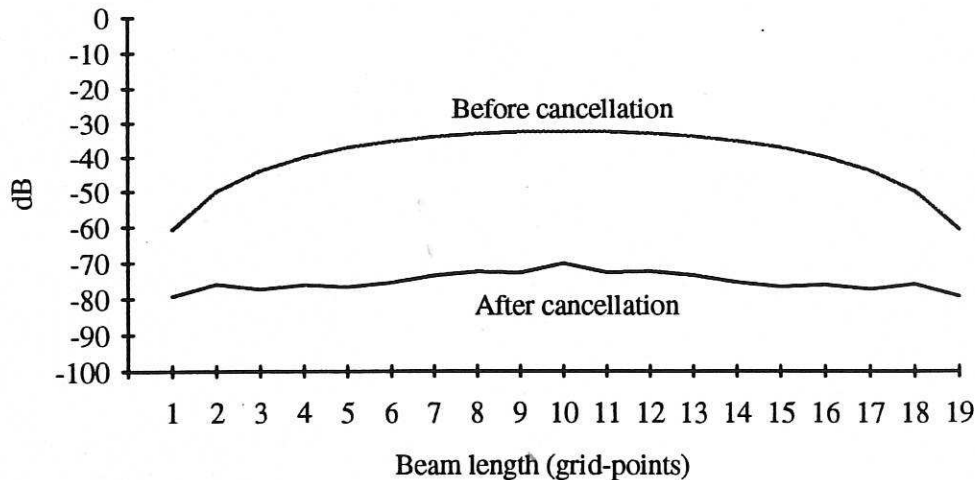


Figure 12: Average autopower spectral densities along the beam before and after cancellation with the SIMO self-tuning AVC system.

The control method developed aims at broadband vibration suppression. The transfer characteristics of the required controller, thus, designed and implemented are continuous frequency-dependent leading to a reduction of all the vibration modes of the structure. An important aspect of the design of the AVC system is the geometrical composition of system components. The stability of the system, due to the feedback loop(s) from the secondary source(s) to the detector, is affected by the location of the detector and secondary source(s) with respect to one another; if these are located so that the loop gain(s) at some frequency is unity then the system will be unstable. The detector in the system is used to gather information on the vibration modes of the system that need to be reduced. This information is then used to generate and apply the control force(s) through the secondary source(s). Thus, it is important to consider the location of the detector from the information gathering viewpoint and the secondary source(s) from the viewpoint of transfer of control energy into the vibration modes of the structure.

A comparison of the performance of the system with the SIMO and SISO controllers reveals that the performance of the system with the SIMO controller is significantly better than that with the SISO controller. This implies that the utilisation of a multiple set of cancelling sources enhances the performance of the system. However, it must be noted that

the geometrical arrangement of system components as discussed earlier plays an important role in the performance of the system.

#### 4 CONCLUSION

The design and implementation of a self-tuning active control system for noise cancellation and vibration suppression has been presented, discussed and verified through simulations. Active control for noise cancellation and vibration suppression utilises the superposition of waves by artificially generating cancelling source(s) to destructively interfere with the unwanted source and thus result in cancellation. An active control mechanism for broadband cancellation of noise and vibration has been developed within an adaptive control framework. The algorithm thus developed and implemented on a digital processor, incorporates on-line design and implementation of the controller in real-time. Moreover, a supervisory level control has been incorporated within the control mechanism allowing on-line monitoring of system performance and controller adaptation. The performance of the algorithm has been verified in the cancellation of broadband noise in a free-field medium and in the suppression of broadband vibration in a flexible beam system. A significant amount of cancellation has been achieved over the full frequency range of the disturbance in each case. It has been noted that the level of cancellation achieved increases with an active control system incorporating a multiple set of cancelling sources. However, for the performance of the system to be robust, the design involving the addition of more sources is to include suitable geometrical compositions of system components.

#### 5 REFERENCES

- Bullmore, A. J., Nelson, P. A., Curtis, A. R. D. and Elliott, S. J. (1987). The active minimization of harmonic enclosed sound fields, Part II: A computer simulation. *Journal of Sound and Vibration*, **117**, (1), pp. 15-33.
- Burgess, J. C. (1981). Active adaptive sound control in a duct: A computer simulation. *Journal of the Acoustical Society of America*, **70**, (3), pp. 715-726.

- Chaplin, B. (1980). The cancellation of repetitive noise and vibration. *Proceedings of Inter-noise 80: International conference on Noise Control Engineering*, Florida, **II**, pp. 699-702.
- Chaplin, B. (1983). Anti-noise - The Essex breakthrough. *Chartered Mechanical Engineering*, **30**, pp. 4107.
- Chaplin, G. B. B. and Smith, R. A. (1981). Active control of repetitive noise and vibration. *Proceedings of the Institute of Acoustics*, February, pp. 9-12.
- Chaplin, G. B. B., Smith, R. A. and Bramer, T. P. C. (1987). Methods and apparatus for reducing repetitive noise entering the ear. *US Patent No. 4 654 871*.
- Clark, R. L. and Fuller, C. R. (1991). Control of sound radiation with adaptive structures. *Journal of Intelligent Systems and structures*, **2**, pp. 431-452.
- Conover, W. B. (1956). Fighting noise with noise. *Noise Control*, **92**, pp. 78-82 & 92.
- Dines, P. J. (1982). Comparison of least squares estimation and impulse response techniques for active control of flame noise. *Proceedings of the Institute of Acoustics*, November, pp. F2.1-F2.4.
- Elliott, S. J. and Nelson, P. A. (1986). An adaptive algorithm for multichannel active control. *Proceedings of the Institute of Acoustics*, **8**, (Part 1), pp. 135-147.
- Elliott, S. J., Curtis, A. R. D., Bullmore, A. J. and Nelson, P. A. (1987a). The active minimization of harmonic enclosed sound fields, Part III: Experimental verification. *Journal of Sound and Vibration*, **117**, (1), pp. 35-58.
- Elliott, S. J., Sothers, I. M. and Nelson, P. A. (1987b). A multiple error LMS algorithm and its application to the active control of sound and vibration. *IEEE Transactions on Acoustics, Speech, and Signal Processing*, **35**, (10), pp. 1423-1434.
- Eriksson, L. J., Allie, M. C. and Greiner, R. A. (1987). The selection and application of an IIR adaptive filter for use in active sound attenuation. *IEEE Transactions on Acoustics, Speech, and Signal Processing*, **35**, (4), pp. 433-437.
- Eriksson, L. J., Allie, M. C., Bremigan, C. D. and Greiner, R. A. (1988). Active noise control using adaptive digital signal processing. *Proceedings of IEEE International Conference on Acoustics, Speech, and Signal Processing*, **5**, pp. 2594-2597.
- Fuller, C. R., Rogers, C. A. and Robertsaw, H. H. (1992). Control of sound radiation with active/adaptive structures. *Journal of Sound and Vibration*, **157**, (1), pp. 19-39.

- Guicking, D. (1993). Active noise control - A review based on patent specifications. In Crocker, M. J. and Ivanov, N. I. (eds.), *Proceedings of Noise-93: International Conference on Noise and Vibration Control*, St Petersburg, 31 May-03 June 1993, Interpublish Ltd, St Petersburg, **2**, pp. 153-157.
- Harris, C. J. and Billings, S. A. (eds). (1981). *Self-tuning and adaptive control: Theory and applications*, Peter Peregrinus, London.
- Hesselman, N. (1978). Investigation of noise reduction on a 100 KVA transformer tank by means of active methods. *Applied Acoustics*, **11**, (1), pp. 27-34.
- Leitch, R. R. and Tokhi, M. O. (1986). The implementation of active noise control systems using digital signal processing techniques. *Proceedings of The Institute of Acoustics*, **8**, (Part 1), pp. 149-157.
- Leitch, R. R. and Tokhi, M. O. (1987). Active noise control systems. *IEE Proceedings-A*, **134**, (6), pp. 525-546.
- Leventhal, H. G. (1980). Active attenuators - A historical review and some recent developments. *Proceedings of Inter-noise 80: International Conference on Noise Control Engineering*, Florida, **II**, pp. 679-682.
- Lueg, P. (1936). Process of silencing sound oscillations. *US Patent 2 043 416*.
- Munjal, M. L. and Eriksson, L. J. (1988). An analytical, one-dimensional, standing-wave model of a linear active noise control system in a duct. *The Journal of the Acoustical Society of America*, **84**, (3), pp. 1086-1093.
- Nelson, P. A., Curtis, A. R. D., Elliott, S. J. and Bullmore, A. J. (1987). The active minimization of harmonic enclosed sound fields, Part I: Theory. *Journal of Sound and Vibration*, **117**, (1), pp. 1-13.
- Ross, C. F. (1978). Experiments on the active control of transformer noise. *Journal of Sound and Vibration*, **61**, (4), pp. 473-480.
- Ross, C. F. (1982). An adaptive digital filter for broadband active sound control. *Journal of Sound and Vibration*, **80**, (3), pp. 381-388.
- Roure, A. (1985). Self-adaptive broadband active sound control system. *Journal of Sound and Vibration*, **101**, (3), pp. 429-441.

- Roure, A. and Nayroles, B. (1984). Autoadaptive broadband active absorption in ducts by the means of transversal filtering. *Proceedings of Inter-noise 84: International conference on Noise Control Engineering*, Honolulu, I, pp. 493-496.
- Sjosten, P. (1985). Experiences of an adaptive control system for active noise control. *Proceedings of Inter-noise 85: International conference on Noise Control Engineering*, Munich, I, pp. 595-598.
- Snyder, S. D. and Hansen, C. H. (1992). Design consideration for active noise control systems implementing the multiple input, multiple output LMS algorithm. *Journal of Sound and Vibration*, **159**, (1), pp. 157-174.
- Tokhi, M. O. (1995). Analysis and robust design of active noise control systems incorporating compact sources. *International Journal of Active Control*, **1**, (2), pp. 109-144.
- Tokhi, M. O. and Leitch, R. R. (1989). Self-tuning active noise control. *IEE Digest No. 1989/46: Colloquium on Adaptive Filtering*, 22 March, London, pp. 9/1-9/4.
- Tokhi, M. O. and Leitch, R. R. (1991a). Design of active noise systems operating in three-dimensional non-dispersive propagation medium. *Noise Control Engineering Journal*, **36**, (1), pp. 41-53.
- Tokhi, M. O. and Leitch, R. R. (1991b). Design and implementation of self-tuning active noise control systems. *IEE Proceedings-D: Control Theory and Applications*, **138**, (5), pp. 421-430.
- Tokhi, M. O. and Leitch, R. R. (1991c). The robust design of active noise control systems based on relative stability measures. *The Journal of The Acoustical Society of America*, **90**, (1), pp. 334-345.
- Tokhi, M. O. and Leitch, R. R. (1992). *Active noise control*, Clarendon Press, Oxford.
- Virk, G. S. and Kourmoulis, P. K. (1988). On the simulation of systems governed partial differential equations. *Proceedings of IEE Conference on Control-88*, pp. 318-321.
- Warnaka, G. E. (1982). Active attenuation of noise: the state of the art. *Noise Control Engineering*, **18**, (3), pp. 100-110.
- Wellstead, P. E. and Zarrop, M. B. (1991). *Self-tuning systems - Control and signal processing*, John Wiley, Chichester.

